A finite volume method for Maxwell's equations with discontinuous physical coefficients

Tsz Shun Chung* and Jun Zou†

Abstract

In this paper, we consider Maxwell's equations in a general three-dimensional polyhedral domain composed of two dialectic materials with different physical parameters. A finite volume method is derived to solve the problem, and a new approach is proposed to handle the physical characteristics of the electromagnetic fields on the interface between the two different materials. The approximate electromagnetic fields are shown to satisfy the two divergence constraints at the discrete level. Numerical examples demonstrate the efficiency of the finite volume method for solving Maxwell's equations with discontinuous physical coefficients and the method can achieve the second order accuracy both in space and time, the same accuracy as the existing finite volume methods for Maxwell's equations with smooth physical coefficients.

1 Introduction

Over past few decades, numerical methods for solving Maxwell's equations in homogeneous media have been well developed. Those methods include finite difference methods [7] [12], finite volume methods [6] [9] [13], and finite element methods [3]. However, for many real applications, such as aerospace design and target identification, one needs to solve Maxwell's equations in inhomogeneous media [4] [7] [11]. The aforementioned numerical methods are either not directly applicable or inefficient (with lower order convergence) for these problems due to different physical characteristics reflected by the electric permittivities and magnetic permeabilities of different media, and the extra interface conditions the electric and magnetic fields need to satisfy on the interface.

Several attempts have been made to handle the interface Maxwell's problems [1] [11] [13]. For example, Yee and Chen [13] studied an FDTD/FVTD hybrid method for the interface problem, assuming both the tangential components of the electric and magnetic fields are continuous across the interface and the electric field is tangentially piecewise constant on the interface. Chen, Du and Zou [1] proposed an edge finite element method for solving the Maxwell's system with very general inhomogeneous interface conditions from some important physical laws and developed a general framework for its convergence analysis. In this paper,

*Department of Mathematics, The Chinese University of Hong Kong, Shatin, Hong Kong.

†Department of Mathematics, The Chinese University of Hong Kong, Shatin, Hong Kong. The work of this author was partially supported by Hong Kong RGC Grants CUHK4004/98P and CUHK4292/00P.

we present a new and simple approach to handle the general interface conditions by a finite volume method. This method converges with a second order accuracy as it is for non-interface problems, and also satisfies two constraint equations at the discrete level.

2 Maxwell's Equations

We next introduce the Maxwell's equations in a physical domain Ω occupied by two different dialectic materials. We shall consider Ω to be a general polyhedral domain. Let $\mathbf{E}$ and $\mathbf{H}$ be the electric and magnetic fields respectively, then the full Maxwell's equations are given by

$$\begin{aligned} \epsilon \mathbf{E}_t - \mathbf{curl}\, \mathbf{H} &= \mathbf{J} \quad \text{in} \quad \Omega \times (0,T), && (2.1)\\ \mu \mathbf{H}_t + \mathbf{curl}\, \mathbf{E} &= 0 \quad \text{in} \quad \Omega \times (0,T), && (2.2)\\ \mathrm{div}(\epsilon \mathbf{E}) &= \rho \quad \text{in} \quad \Omega \times (0,T), && (2.3)\\ \mathrm{div}(\mu \mathbf{H}) &= 0 \quad \text{in} \quad \Omega \times (0,T). && (2.4) \end{aligned}$$

Here $\mathbf{J}(x,t)$ is the known applied current density and $\rho(x,t)$ is the charge density. Let Ω_1 be a polyhedral region lying strictly inside Ω. We denote its boundary by $\Gamma = \partial\Omega_1$ and the unit outward normal on Γ by $\mathbf{m}$, and let $\Omega_2 = \Omega \backslash \bar{\Omega}_1$. Assume that Ω_1 and Ω_2 are occupied by two different dialectic materials, so the parameters ϵ and μ are discontinuous across the interface Γ. For the ease of notation, we consider the case that ϵ and μ are piecewise constant functions in Ω, i.e., $\epsilon = \epsilon_i$ and $\mu = \mu_i$ in Ω_i for $i = 1, 2$. Here ϵ_i and μ_i are positive constants[1]. We suppose the perfect conductor boundary condition:

$$\mathbf{E} \times \mathbf{n} = 0 \quad \text{on} \quad \partial\Omega \times (0,T) \tag{2.5}$$

where $\mathbf{n}$ is the unit outward normal on $\partial\Omega$. Throughout the paper, the jump of any function A across the interface Γ is defined as $[A] := A_2|_\Gamma - A_1|_\Gamma$, where $A_1 = A|_{\Omega_1}$ and $A_2 = A|_{\Omega_2}$. It is known physically that the electric and magnetic fields $\mathbf{E}$ and $\mathbf{H}$ satisfy the following jump conditions on the interface Γ:

$$\begin{aligned} [\mathbf{E} \times \mathbf{m}] = 0 \quad , \quad [\epsilon \mathbf{E} \cdot \mathbf{m}] = \rho_\Gamma, && (2.6)\\ [\mathbf{H} \times \mathbf{m}] = \mathbf{J}_\Gamma \quad , \quad [\mu \mathbf{H} \cdot \mathbf{m}] = 0, && (2.7) \end{aligned}$$

where $\rho_\Gamma(x,t)$ is the surface charge density while $\mathbf{J}_\Gamma(x,t)$ is the surface current density. In addition, we have the following constitutive relations

$$\mathbf{D} = \epsilon \mathbf{E}, \quad \mathbf{B} = \mu \mathbf{H}, \tag{2.8}$$

where $\mathbf{D}$ and $\mathbf{B}$ are the electric and magnetic flux densities respectively.

[1] Our subsequent numerical method can be easily generalized to the case that the parameters ϵ and μ are both piecewise smooth functions

3 Discrete vector fields

We now discuss the triangulation of the domain Ω. Most notations used below are borrowed from Nicolaides, Wang and Wu [8] [9] [10], where a finite volume method was proposed for solving Maxwell's equations with continuous coefficients, i.e., non-inferface problems. We will use the Voronoi-Delaunay triangulation, which has some useful properties that allow us to derive a second order numerical scheme in the subsequent sections.

We first triangulate Ω by using the standard tetrahedral elements, which are called the *primal elements*. This triangulation is chosen so that the faces of the primal elements align with the interface Γ. A primal element with as least one face lying on Γ is called an *interface primal element*. Similarly, a primal face (edge) lying on Γ is called an interface primal face (edge). We assume that all dihedral angles of each tetrahedron are acute.

The *dual elements* are formed by connecting the circumcenters of adjacent primal elements. It is easy to see that all dual elements are convex polyhedra with convex polygonal faces. Note that there are some dual elements (faces and edges), which are separated by the interface Γ into two parts. These are called the interface dual elements (faces and edges). By the geometrical knowledge, we know the following relations between the primal and dual meshes. First, each primal edge is perpendicular to and in one-to-one correspondence with a dual face. Secondly, each dual edge is perpendicular to and in one-to-one correspondence with a primal face. These relations are the key to the derivation of our numerical schemes.

Let N and L be the numbers of primal and dual elements respectively, and F be the number of primal faces (dual edges) and M be the number of primal edges (dual faces). Assume that these quantities are numbered sequentially in some order. The individual elements, faces, edges and nodes of the primal mesh are denoted by τ_i, κ_j, σ_k and ν_l respectively. Those quantities related to the dual mesh are denoted by the primed forms such as τ_i', κ_j', σ_k' and ν_l'. A direction is assigned to each primal and dual edge by the rule that positive direction is from low to high node number. Direction is also assigned to each primal (dual) face such that it is the same as the corresponding dual (primal) edge. We denote by F_1 the number of interior primal faces (dual edges) and M_1 the number of interior primal edges (dual faces). For each dual edge σ_j' of length h_j', we define a scaled length:

$$\bar{h}_j' = \begin{cases} \frac{1}{\mu_1} h_j' & \text{if} \quad \sigma_j' \in \Omega_1 \\ \frac{1}{\mu_2} h_j' & \text{if} \quad \sigma_j' \in \Omega_2 \\ (\frac{1}{\mu_1} a_j + \frac{1}{\mu_2}(1 - a_j)) h_j' & \text{otherwise,} \end{cases}$$

where $0 < a_j < 1$ is the ratio of the length of the portion of σ_j' that belongs to Ω_1 over the length of σ_j'. For any u and v in $\mathbb{R}^{F_1}$, we introduce a mesh and parameter depending inner product defined by

$$(u, v)_W := \sum_{\kappa_j \in \Omega} u_j v_j s_j \bar{h}_j' = (Su, D'v) = (D'u, Sv), \tag{3.1}$$

where $S := \text{diag}(s_j)$ and $D' := \text{diag}(\bar{h}_j')$ are $F_1 \times F_1$ diagonal matrices, $(\cdot, \cdot)$ denotes the standard Euclidean inner product. Similarly, for each dual face κ_j' with area s_j', we define a

scaled area:

$$\bar{s}'_j = \begin{cases} \epsilon_1 s'_j & \text{if} \quad \kappa'_j \in \Omega_1 \\ \epsilon_2 s'_j & \text{if} \quad \kappa'_j \in \Omega_2 \\ (\epsilon_1 b_j + \epsilon_2(1-b_j)) s'_j & \text{otherwise,} \end{cases}$$

where $0 < b_j < 1$ is the ratio of the area of the portion of κ'_j that belongs to Ω_1 over the area of κ'_j. Also, we define a mesh and parameter depending inner product in $\mathbb{R}^{M_1}$ by

$$(u, v)_{W'} := \sum_{\kappa'_j \in \Omega} u_j v_j \bar{s}'_j h_j = (S'u, Dv) = (Du, S'v), \tag{3.2}$$

where $S' := \mathrm{diag}(\bar{s}'_j)$ and $D := \mathrm{diag}(h_j)$ are $M_1 \times M_1$ diagonal matrices.

For any $\sigma_j \in \partial\kappa_i$, we say σ_j is oriented positively along $\partial\kappa_i$ if the direction of σ_j agrees with the direction of κ_i by the right hand rule with the thumb pointing to the direction of the dual edge σ'_i. Otherwise, we say σ_j is oriented negatively along $\partial\kappa_i$. For each interior primal face κ_i, we define its discrete circulation by

$$(Cu)_{\kappa_i} := \sum_{\sigma_j \in \partial\kappa_i} u_j \tilde{h}_j, \tag{3.3}$$

where $\tilde{h}_j = h_j$ if σ_j is oriented positively along $\partial\kappa_i$; and $\tilde{h}_j = -h_j$ otherwise. Similarly, we define a discrete circulation for each interior dual face κ'_i by

$$(C'u)_{\kappa'_i} := \sum_{\sigma'_j \in \partial\kappa'_i} u_j \tilde{h}'_j, \tag{3.4}$$

where $\tilde{h}'_j = \bar{h}'_j$ if σ'_j is oriented postively along $\partial\kappa'_i$; and $\tilde{h}'_j = -\bar{h}'_j$ otherwise.

We remark that (3.3) and (3.4) are the discrete analog of the following integrals

$$\int_{\kappa_i} \mathrm{curl}\, \mathbf{E} \cdot \mathbf{n}_i \, d\sigma \quad \text{and} \quad \int_{\kappa'_i} \mathrm{curl}\, \mathbf{H} \cdot \mathbf{n}_i \, d\sigma$$

by the Stokes' theorem. Here and below, $\mathbf{n}_i$ and $\mathbf{t}_i$ denote the unit normal and tangential direction of the corresponding face and edge respectively.

Let τ_i be a primal element and $\kappa_j \in \partial\tau_i$ be a primal face. We say κ_j is oriented positively along $\partial\tau_i$ if the dual edge σ'_j on κ_j is directed toward the outside of τ_i. Otherwise we say κ_j is oriented negatively along $\partial\tau_i$. For each primal element τ_i, we define a discrete flux by

$$(\mathcal{D}u)_i := \sum_{\kappa_j \in \partial\tau_i} u_j \tilde{s}_j, \qquad \forall u \in \mathbb{R}^{F_1} \tag{3.5}$$

where no components of u related to the boundary faces are involved, and $\tilde{s}_j = s_j$ if κ_j is oriented positively along $\partial\tau_i$; and $\tilde{s}_j = -s_j$ otherwise. Note that the mapping $\mathcal{D}$ is the discrete version of the divergence operator by noting that

$$\int_{\tau_i} \mathrm{div}\, \mathbf{u} \, dx = \int_{\partial\tau_i} \mathbf{u} \cdot \mathbf{n} \, ds.$$

Similarly, for each dual element τ_i', we define a discrete flux by

$$(\mathcal{D}'u)_i := \sum_{\kappa_j' \in \partial \tau_i'} u_j \tilde{s}_j', \quad \forall u \in \mathbb{R}^{M_1} \tag{3.6}$$

where $\tilde{s}_j' = \bar{s}_j'$ if κ_j' is oriented positively along $\partial\tau_i'$; and $\tilde{s}_j' = -\bar{s}_j'$ otherwise.

Next, we present a discrete analog of the identity $\mathrm{div}(\mathbf{curl}\,\mathbf{u}) = 0$. To do so, we first introduce two matrices B and B'. B is a $F_1 \times N$ matrix given by

$$B_{ji} := \begin{cases} 1 & \text{if } \kappa_j \text{ is oriented postively along } \partial\tau_i \\ -1 & \text{if } \kappa_j \text{ is oriented negatively along } \partial\tau_i \\ 0 & \text{if } \kappa_j \text{ does not meet } \partial\tau_i, \end{cases}$$

while B' is a $M_1 \times L$ matrix given by

$$B'_{ji} := \begin{cases} 1 & \text{if } \kappa_j' \text{ is oriented postively along } \partial\tau_i' \\ -1 & \text{if } \kappa_j' \text{ is oriented negatively along } \partial\tau_i' \\ 0 & \text{if } \kappa_j' \text{ does not meet } \partial\tau_i'. \end{cases}$$

Lemma 1 *We have*

$$\mathcal{D} = B^T S\,, \qquad B^T C = 0\,; \tag{3.7}$$

$$\mathcal{D}' = (B')^T S'\,, \qquad (B')^T C' = 0. \tag{3.8}$$

Proof. For any $u \in \mathbb{R}^{F_1}$, we have

$$(\mathcal{D}u)_i = \sum_{\kappa_j \in \partial\tau_i} u_j \tilde{s}_j = \sum_{j=1}^{F_1} d_j u_j s_j$$

where

$$d_j = \begin{cases} 1 & \text{if } \kappa_j \text{ is oriented positively along } \partial\tau_i \\ -1 & \text{if } \kappa_j \text{ is oriented negatively along } \partial\tau_i \\ 0 & \text{if } \kappa_j \text{ does not meet } \partial\tau_i. \end{cases}$$

Clearly, the vector formed by d_j's is the i-th column of the matrix B and hence $\mathcal{D} = B^T S$. The relation $\mathcal{D}' = (B')^T S'$ can be proved similarly.

For (3.8), we observe that the i-th row of B^T is the direction of κ_j with respect to τ_i. Let $w \in \mathbb{R}^M$ with $w|_{\partial\Omega} = 0$. Then in the i-th component of $B^T C w$, each w_j which is involved in that component appears exactly twice with two opposite signs, hence $(B^T C w)_i = 0$. Similar argument can be applied to show $(B')^T C' = 0$. □

4 Finite volume method

In this section we present a finite volume method for solving the Maxwell's equations (2.1)-(2.4). In this finite volume scheme, we will approximate the edge average of $\mathbf{E}$ on each primal edge and the face average of $\mathbf{B}$ on each primal face. Note that we choose the magnetic flux

density $\mathbf{B}$ for the approximation, not the magnetic field $\mathbf{H}$ which is used in the most existing methods. This is one of the crucial observations for our method to achieve the same accuracy as the most efficient finite volume methods for the Maxwell's equations with smooth physical coefficients.

We now introduce some average quantities. For the magnetic flux density $\mathbf{B}$, we define its primal face average $B_f \in \mathbb{R}^{F_1}$ by

$$(B_f)_i := \frac{1}{s_i} \int_{\kappa_i} \mathbf{B} \cdot \mathbf{n}_i \, d\sigma$$

for each primal face κ_i, and its dual edge average $B'_e \in \mathbb{R}^{F_1}$ by

$$(B'_e)_i := \frac{1}{h'_i} \int_{\sigma'_i} \mathbf{B} \cdot \mathbf{t}_i \, dl$$

for each non-interface dual edge σ'_i and

$$(B'_e)_i := \alpha_i \frac{1}{h_i^1} \int_{\sigma_i^1} \mathbf{B} \cdot \mathbf{t}_i \, dl + (1-\alpha_i) \frac{1}{h_i^2} \int_{\sigma_i^2} \mathbf{B} \cdot \mathbf{t}_i \, dl$$

for each interface dual edge σ'_i. Here $\sigma_i^1 = \sigma'_i \cap \Omega_1$ and $\sigma_i^2 = \sigma'_i \cap \Omega_2$ are the portions of σ'_i in Ω_1 and Ω_2 respectively, and $\alpha_i := \mu_1^{-1} h_i^1 (\bar{h}'_i)^{-1}$ with h_i^r being the length of σ_i^r for $r = 1, 2$.

For the electric field $\mathbf{E}$, we define its primal edge average $E_e \in \mathbb{R}^{M_1}$ by

$$(E_e)_i := \frac{1}{h_i} \int_{\sigma_i} \mathbf{E} \cdot \mathbf{n}_i \, dl$$

for each primal edge σ_i, and its dual face average $E'_f \in \mathbb{R}^{M_1}$ by

$$(E'_f)_i := \frac{1}{s'_i} \int_{\kappa'_i} \mathbf{E} \cdot \mathbf{n}_i \, d\sigma$$

for each non-interface dual face κ'_i and

$$(E'_f)_i := \beta_i \frac{1}{s_i^1} \int_{\kappa_i^1} \mathbf{E} \cdot \mathbf{n}_i \, d\sigma + (1-\beta_i) \frac{1}{s_i^2} \int_{\kappa_i^2} \mathbf{E} \cdot \mathbf{n}_i \, d\sigma$$

for each interface dual face κ'_i. Here $\kappa_i^1 = \kappa'_i \cap \Omega_1$ and $\kappa_i^2 = \kappa'_i \cap \Omega_2$ are the portions of κ'_i in Ω_1 and Ω_2 with their areas being s_i^1 and s_i^2 respectively, and $\beta_i := \epsilon_1 s_i^1 (\bar{s}'_i)^{-1}$.

Now, we are ready to derive our finite volume method. First, integrating both sides of (2.2) on a primal face κ_j and apply the Stokes' theorem, we obtain

$$\frac{d}{dt} \int_{\kappa_j} \mathbf{B} \cdot \mathbf{n}_j \, d\sigma + \sum_{\sigma_i \in \partial \kappa_j} \int_{\sigma_i} \mathbf{E} \cdot \mathbf{t}_i \, dl = 0,$$

where the directions $\mathbf{t}'_i s$ are defined by the right hand rule on the face κ_j. By the definition of face and edge averages, this can be written as

$$\frac{d}{dt}((B_f)_j s_j) + (CE_e)_{\kappa_j} = 0. \tag{4.1}$$

Secondly, integrating both sides of (2.1) on a non-interface dual face $\kappa_j' \in \Omega_r$ $(r = 1, 2)$, we obtain

$$\frac{d}{dt}\int_{\kappa_j'} \epsilon_r \mathbf{E}\cdot\mathbf{n}_j \, d\sigma - \sum_{\sigma_i'\in\partial\kappa_j'} \int_{\sigma_i'} \frac{1}{\mu_i}\mathbf{B}\cdot\mathbf{t}_i \, dl = \int_{\kappa_j'} \mathbf{J}\cdot\mathbf{n}_j \, d\sigma,$$

By the definitions of $\tilde{h}_j'$ and $\bar{s}_j'$, this can be written as

$$\frac{d}{dt}((E_f')_j \bar{s}_j') - (C'B_e')_{\kappa_j'} = \int_{\kappa_j'} \mathbf{J}\cdot\mathbf{n}_j \, d\sigma. \tag{4.2}$$

Finally, we consider an interface dual face κ_j', divided by the interface Γ into two parts κ_j^1 and κ_j^2, see Figure 1. Integrating both sides of (2.1) on κ_j', we have

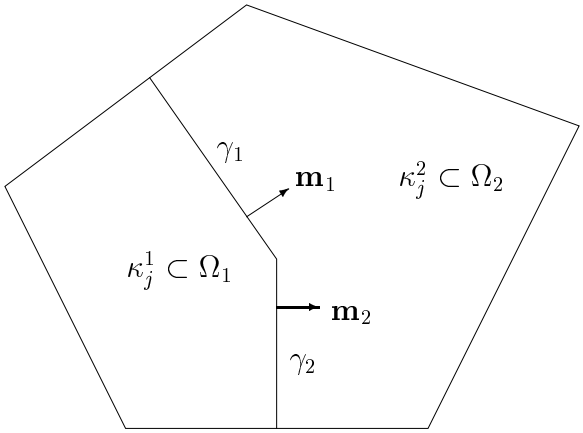

Figure 1: A dual face κ_j', divided by the interface into two parts κ_j^1, κ_j^2

$$\sum_{r=1}^{2}\frac{d}{dt}\int_{\kappa_j^r} \epsilon_r \mathbf{E}\cdot\mathbf{n}_j \, d\sigma - \sum_{r=1}^{2}\int_{\kappa_j^r} \mathbf{curl}\,\mathbf{H}\cdot\mathbf{n}_j \, d\sigma = \int_{\kappa_j'} \mathbf{J}\cdot\mathbf{n}_j \, d\sigma.$$

Applying Stokes' theorem and the relation $\mathbf{B} = \mu\mathbf{H}$, we have

$$\begin{aligned}&\frac{d}{dt}\int_{\kappa_j^1} \epsilon_1 \mathbf{E}\cdot\mathbf{n}_j \, d\sigma + \frac{d}{dt}\int_{\kappa_j^2} \epsilon_2 \mathbf{E}\cdot\mathbf{n}_j \, d\sigma \\ &\quad - \sum_{\sigma_i'\in\partial\kappa_j^1}\int_{\sigma_i'} \frac{1}{\mu_1}\mathbf{B}\cdot\mathbf{t}_i^1 \, dl - \sum_{\sigma_i'\in\partial\kappa_j^2}\int_{\sigma_i'} \frac{1}{\mu_2}\mathbf{B}\cdot\mathbf{t}_i^2 \, dl = \int_{\kappa_j'} \mathbf{J}\cdot\mathbf{n}_j \, d\sigma\,.\end{aligned} \tag{4.3}$$

We remark that there are some edges of κ_j^r $(r = 1, 2)$, that belong to Γ but are not the edges of our primal and dual meshes, see γ_1 and γ_2 in Figure 1. It is easy to see that

$$\begin{aligned}\sum_{\sigma_i'\in\partial\kappa_j^1}\int_{\sigma_i'} \frac{1}{\mu_1}\mathbf{B}\cdot\mathbf{t}_i^1 \, dl &= \sum_{\sigma_i'\in\partial\kappa_j^1\setminus\Gamma}\int_{\sigma_i'} \frac{1}{\mu_1}\mathbf{B}_1\cdot\mathbf{t}_i^1 \, dl + \int_{\gamma_1}\frac{1}{\mu_1}\mathbf{B}_1\cdot\mathbf{t}_i^1 \, dl + \int_{\gamma_2}\frac{1}{\mu_1}\mathbf{B}_1\cdot\mathbf{t}_i^1 \, dl\,,\\ \sum_{\sigma_i'\in\partial\kappa_j^2}\int_{\sigma_i'} \frac{1}{\mu_2}\mathbf{B}\cdot\mathbf{t}_i^2 \, dl &= \sum_{\sigma_i'\in\partial\kappa_j^2\setminus\Gamma}\int_{\sigma_i'} \frac{1}{\mu_2}\mathbf{B}_2\cdot\mathbf{t}_i^2 \, dl + \int_{\gamma_1}\frac{1}{\mu_2}\mathbf{B}_2\cdot\mathbf{t}_i^2 \, dl + \int_{\gamma_2}\frac{1}{\mu_2}\mathbf{B}_2\cdot\mathbf{t}_i^2 \, dl\end{aligned}$$

where $\mathbf{B}_i = \mathbf{B}|_{\Omega_i}$ for $i = 1, 2$. Let $\tilde{\mathbf{t}}_1$ and $\tilde{\mathbf{t}}_2$ be the directions of γ_1 and γ_2 respectively, then summing up the above two equations we obatin the right-hand side of the resulting equation:

$$\sum_{r=1}^{2} \sum_{\sigma_i' \in \Omega_r} \int_{\sigma_i'} \frac{1}{\mu_r} \mathbf{B} \cdot \mathbf{t}_i \, dl + \sum_{\sigma_i' \cap \Gamma \neq \phi} \left(\int_{\sigma_i' \cap \Omega_1} \frac{1}{\mu_1} \mathbf{B}_1 \cdot \mathbf{t}_i \, dl + \int_{\sigma_i' \cap \Omega_2} \frac{1}{\mu_2} \mathbf{B}_2 \cdot \mathbf{t}_i \, dl \right)$$
$$+ \int_{\gamma_1} (\mathbf{H}_2 - \mathbf{H}_1) \cdot \tilde{\mathbf{t}}_1 \, dl + \int_{\gamma_2} (\mathbf{H}_2 - \mathbf{H}_1) \cdot \tilde{\mathbf{t}}_2 \, dl,$$

By geometry and interface conditions, we have

$$(\mathbf{H}_2 - \mathbf{H}_1) \cdot \tilde{\mathbf{t}}_1 = ((\mathbf{H}_2 - \mathbf{H}_1) \times \mathbf{m}_1) \cdot \mathbf{n}_j = \mathbf{J}_\Gamma \cdot \mathbf{n}_j \,, \tag{4.4}$$
$$(\mathbf{H}_2 - \mathbf{H}_1) \cdot \tilde{\mathbf{t}}_2 = ((\mathbf{H}_2 - \mathbf{H}_1) \times \mathbf{m}_2) \cdot \mathbf{n}_j = \mathbf{J}_\Gamma \cdot \mathbf{n}_j, \tag{4.5}$$

Collecting these results, (4.3) becomes,

$$\frac{d}{dt} \int_{\kappa_j^1} \epsilon_1 \mathbf{E} \cdot \mathbf{n}_j \, d\sigma + \frac{d}{dt} \int_{\kappa_j^2} \epsilon_2 \mathbf{E} \cdot \mathbf{n}_j \, d\sigma - \sum_{r=1}^{2} \sum_{\sigma_i' \in \Omega_r} \int_{\sigma_i'} \frac{1}{\mu_r} \mathbf{B} \cdot \mathbf{t}_i \, dl$$
$$- \sum_{\sigma_i' \cap \Gamma \neq \phi} \left(\int_{\sigma_i^1} \frac{1}{\mu_1} \mathbf{B}_1 \cdot \mathbf{t}_i \, dl + \int_{\sigma_i^2} \frac{1}{\mu_2} \mathbf{B}_2 \cdot \mathbf{t}_i \, dl \right)$$
$$= \int_{\kappa_j'} \mathbf{J} \cdot \mathbf{n}_j \, d\sigma + \sum_{r=1}^{2} \int_{\gamma_r} \mathbf{J}_\Gamma \cdot \mathbf{n}_j \, dl \,,$$

where $\sigma_i^r = \sigma_i' \cap \Omega_r$, $r = 1, 2$. By the definition of the interface face and edge averages, we can write this as

$$\frac{d}{dt}((E_f')_j \bar{s}_j') - (C' B_e')_{\kappa_j'} = \int_{\kappa_j'} \mathbf{J} \cdot \mathbf{n}_j \, d\sigma. + \sum_{r=1}^{2} \int_{\gamma_r} \mathbf{J}_\Gamma \cdot \mathbf{n}_j \, dl \,. \tag{4.6}$$

The other interface dual faces can be handled in a similar manner.

Now let $E \in \mathbb{R}^{M_1}$ and $B \in \mathbb{R}^{F_1}$ be the approximations of the primal edge and face averages of the true solution $\mathbf{E}$ and $\mathbf{B}$ to (2.1)-(2.4) respectively. Then (4.1) suggests

$$s_j \frac{dB_j}{dt} + (CE)_j = 0. \tag{4.7}$$

Noting the fact that each dual face (edge) average and the corresponding primal edge (face) average are approximately the same as h is sufficiently small. It is important to observe that this fact is also true for the interface dual faces and edges due to the interface conditions that $\mathbf{E}$ is tangentially continuous while $\mathbf{B}$ is normally continuous across the interface Γ. With this fact and the equations (4.2) and (4.6), we naturally come to the following approximations:

$$\bar{s}_j' \frac{dE_j}{dt} - (C'B)_j = \int_{\kappa_j'} \mathbf{J} \cdot \mathbf{n}_j \, d\sigma \tag{4.8}$$

for non-interface dual faces κ_j' and

$$\bar{s}_j' \frac{dE_j}{dt} - (C'B)_j = \int_{\kappa_j'} \mathbf{J} \cdot \mathbf{n}_j \, d\sigma + \sum_{r=1}^{2} \int_{\gamma_r} \mathbf{J}_\Gamma \cdot \mathbf{n}_j \, dl \tag{4.9}$$

for interface dual faces κ_j'. This leads to the following semi-discrete scheme:

Find $E \in \mathbb{R}^{M_1}$ and $B \in \mathbb{R}^{F_1}$ such that

$$S'\frac{dE}{dt} - C'B = \tilde{J}, \tag{4.10}$$

$$S\frac{dB}{dt} + CE = 0 \tag{4.11}$$

where $\tilde{J} \in \mathbb{R}^{M_1}$ are defined by the right-hand sides of (4.8) or (4.9). Note that S and S' are both diagonal matrices and hence are easy to invert.

To further discretize the system (4.10)-(4.11) in time, we apply the usual leapfrog scheme [12]. Divide $[0, T]$ into N_T equal subintervals and let Δt be the length of each subinterval. Denote $t_n := n\Delta t$, for $0 \le n \le N_T$. Then we approximate the true solution $\mathbf{E}(t)$ at t_n by E^n while the true solution $\mathbf{B}(t)$ at $t_{n+\frac{1}{2}}$ by $B^{n+\frac{1}{2}}$. The initial condition $B^{\frac{1}{2}}$ is computed by using Taylor's expansion and the Maxwell's equations (2.1)-(2.2).

Using the central difference scheme to discretize the equation (4.10) at time $t = t_{n+\frac{1}{2}}$ and the equation (4.11) at $t = t_{n+1}$, we obtain

$$\begin{aligned} S'\frac{E^{n+1} - E^n}{\Delta t} - C'B^{n+\frac{1}{2}} &= \frac{1}{\Delta t}\int_{t_n}^{t_{n+1}} \tilde{J}(t)\, dt, \\ S\frac{B^{n+\frac{3}{2}} - B^{n+\frac{1}{2}}}{\Delta t} + CE^{n+1} &= 0. \end{aligned}$$

This gives our fully discrete scheme: Given $(E^n, B^{n+\frac{1}{2}})$, the next approximation $(E^{n+1}, B^{n+\frac{3}{2}})$ is calculated directly from the following equations

$$S'(E^{n+1} - E^n) - \Delta t C'B^{n+\frac{1}{2}} = \int_{t_n}^{t_{n+1}} \tilde{J}(t)\, dt, \tag{4.12}$$

$$S(B^{n+\frac{3}{2}} - B^{n+\frac{1}{2}}) + \Delta t CE^{n+1} = 0. \tag{4.13}$$

5 Stability and discrete divergence constraints

In this section we show that our finite volume method (4.12)-(4.13) is stable, and its solution E and B satisfy the two divergence constraint equations (2.3)-(2.4) at the discrete level, if these two constraints are satisfied initially, namely

$$\mathrm{div}(\epsilon\mathbf{E}(x,0)) = \rho(x,0), \quad \mathrm{div}(\mu\mathbf{H}(x,0)) = 0. \tag{5.1}$$

Theorem 1 *Let $B^{n+\frac{1}{2}}$, for $0 \le n \le N_T - 1$, be the solution to the fully discrete scheme (4.12)-(4.13), then $B^{n+\frac{1}{2}}$ is divergence-free at the discrete level, namely, the following holds for $0 \le n \le N_T - 1$:*

$$\mathcal{D}B^{n+\frac{1}{2}} = 0. \tag{5.2}$$

Proof. By Lemma 1 and (4.13), we have

$$\mathcal{D}(B^{n+\frac{3}{2}} - B^{n+\frac{1}{2}}) = B^T S(B^{n+\frac{3}{2}} - B^{n+\frac{1}{2}}) = -\Delta t B^T CE^{n+1} = 0. \tag{5.3}$$

Taking the divergence in both sides of (2.2), we obtain

$$\frac{\partial}{\partial t}\mathrm{div}(\mu\mathbf{H}) = 0,$$

that implies $\mathrm{div}(\mu\mathbf{H}) = 0$ at time $t = \frac{1}{2}\Delta t$ by (5.1). Integrating this equation over a primal element τ_i and using the Stokes' theorem lead to (at $t = \frac{1}{2}\Delta t$)

$$\sum_{\kappa_j \in \partial\tau_i} \int_{\kappa_j} \mathbf{B}\cdot\mathbf{n}_j \, d\sigma = 0.$$

By the definition of B_f, this can be written as

$$(\mathcal{D}B_f^{\frac{1}{2}})_i = 0$$

for any i. Now (5.2) follows from (5.3) and the fact that $B^{\frac{1}{2}} = B_f^{\frac{1}{2}}$. $\square$

Theorem 2 *Let E^n, $0 \le n \le N_T - 1$, be the solution to the fully discrete scheme (4.12)-(4.13), then the divergence constraint (2.3) holds for E^n in the following discrete sense:*

$$\mathcal{D}'E^n = \tilde{\rho}^n + e, \qquad 0 \le n \le N_T - 1 \tag{5.4}$$

e is a vector in $\mathbb{R}^L$ and converges to 0 as h tends to 0, and $\tilde{\rho}$ is a vector in $\mathbb{R}^L$ with its components given by

$$\tilde{\rho}_j^n := \int_{\tau_j'} \rho(x,t_n)\, dx + \int_{\tau_j'\cap\Gamma} \rho_\Gamma(x,t_n)\, d\sigma\,. \tag{5.5}$$

Proof. By Lemma 1 and (4.12), we have for $0 \le n \le N_T - 2$ that

$$\begin{aligned}\mathcal{D}'(E^{n+1} - E^n) &= (B')^T S'(E^{n+1} - E^n) = \Delta t (B')^T C' B^{n+\frac{1}{2}} + (B')^T \tilde{J}^{n+\frac{1}{2}} \\ &= (B')^T \tilde{J}^{n+\frac{1}{2}} = \int_{t_n}^{t_{n+1}} (B')^T \tilde{J}\, dt.\end{aligned}$$

Summing up all these equations over n, we obtain

$$\mathcal{D}'E^n = \mathcal{D}'E^0 + \int_0^{t_n} (B')^T \tilde{J}\, dt, \qquad 0 \le n \le N_T - 1. \tag{5.6}$$

Integrating the initial condition $\mathrm{div}(\epsilon\mathbf{E}(x,0)) = \rho(x,0)$ over an interior dual element τ_i', we have

$$\sum_{\kappa_r' \in \partial\tau_i'} \int_{\kappa_r'} \epsilon\mathbf{E}(x,0)\cdot\mathbf{n}_r \, d\sigma = \int_{\tau_i'} \rho(x,0)\, dx, \tag{5.7}$$

which, by the definition of the face average, can be written as

$$(\mathcal{D}'(E')_f^0)_i = \int_{\tau_i'} \rho(x,0)\, dx. \tag{5.8}$$

Noting $E^0 = E^0_e$ for all primal edges corresponding to the dual faces of τ'_i, (5.8) is equivalent to

$$(\mathcal{D}'E^0)_i = \int_{\tau'_i} \rho(x,0)\, dx + e_i$$

where $e_i := (\mathcal{D}'(E^0_e - (E')^0_f))_i$.

Now for an interface dual element τ'_j, that is $\tau'_j \cap \Gamma \neq \phi$, we can write

$$\int_{\tau'_i} \mathrm{div}(\epsilon \mathbf{E}(x,0))\, dx = \sum_{k=1}^{2} \int_{\tau'_j \cap \Omega_k} \mathrm{div}(\epsilon \mathbf{E}(x,0))\, dx = \int_{\tau'_j} \rho(x,0)\, dx.$$

By the divergence theorem and the jump condition $[\epsilon \mathbf{E} \cdot \mathbf{m}] = \rho_\Gamma$ on Γ, we obtain

$$(\mathcal{D}'E^0)_j = \int_{\tau'_j} \rho(x,0)\, dx + \int_{\tau'_j \cap \Gamma} \rho_\Gamma(x,0)\, d\sigma + e_j,$$

where

$$e_j := ((B')^T[\epsilon_1 s^1_k (E^0_e - E^0_{f^1_k}) + \epsilon_2 s^2_k (E^0_e - E^0_{f^2_k})])_j, \tag{5.9}$$

and $E^0_{f^1_k}$ and $E^0_{f^2_k}$ are the averages of $\mathbf{E}(x,0)$ on the two parts f^1_k and f^2_k of an interface dual face $\kappa'_k \in \partial\tau'_j$ in Ω_1 and Ω_2 respectively.

By the continuity equation $\frac{\partial \rho}{\partial t} = \mathrm{div}\mathbf{J}$, for any interface dual element τ'_j, we have

$$\frac{\partial}{\partial t} \int_{\tau'_j} \rho\, dx = \int_{\tau'_j} \mathrm{div}\mathbf{J}\, dx = \sum_{k=1}^{2} \int_{\tau'_j \cap \Omega_k} \mathrm{div}\mathbf{J}\, dx\,.$$

Applying the divergence theorem,

$$\frac{\partial}{\partial t} \int_{\tau'_j} \rho\, dx = \sum_{\kappa'_r \in \partial\tau'_j} \int_{\kappa'_r} \mathbf{J} \cdot \mathbf{n}_r\, d\sigma - \int_{\tau'_j \cap \Gamma} [\mathbf{J} \cdot \mathbf{m}]\, d\sigma.$$

From equation (2.1), we see

$$\begin{aligned}\int_{\tau'_j \cap \Gamma} [\mathbf{J} \cdot \mathbf{m}]\, d\sigma &= -\int_{\tau'_j \cap \Gamma} [\mathbf{curl}\, \mathbf{H} \cdot \mathbf{m}]\, d\sigma + \frac{\partial}{\partial t} \int_{\tau'_j \cap \Gamma} [\epsilon \mathbf{E} \cdot \mathbf{m}]\, d\sigma \\ &= -\int_{\tau'_j \cap \Gamma} [\mathbf{curl}\, \mathbf{H} \cdot \mathbf{m}]\, d\sigma + \frac{\partial}{\partial t} \int_{\tau'_j \cap \Gamma} \rho_\Gamma\, d\sigma.\end{aligned}$$

From Figure 2 and the equations (4.4)-(4.5),

$$\int_{\tau'_j \cap \Gamma} [\mathbf{curl}\, \mathbf{H} \cdot \mathbf{m}]\, d\sigma = \sum_{\gamma'_r \in \partial(\tau'_j \cap \Gamma)} \int_{\gamma'_r} [\mathbf{H} \cdot \mathbf{t}_r]\, dl = \sum_{\gamma'_r \in \partial(\tau'_j \cap \Gamma)} \int_{\gamma'_r} \mathbf{J}_\Gamma \cdot \mathbf{n}_r\, d\sigma.$$

Combining the above results, we have

$$\frac{\partial}{\partial t} \int_{\tau'_j} \rho\, dx = ((B')^T \tilde{J})_j - \frac{\partial}{\partial t} \int_{\tau'_j \cap \Gamma} \rho_\Gamma\, d\sigma.$$

Integrating both sides over $[0, t_n]$ gives

$$\int_{\tau_j'} \rho(x, t_n)\, dx - \int_{\tau_j'} \rho(x, 0)\, dx = \int_0^{t_n} ((B')^T \tilde{J})_j\, dt + \int_{\tau_j' \cap \Gamma} \rho_\Gamma(x, 0)\, d\sigma - \int_{\tau_j' \cap \Gamma} \rho_\Gamma(x, t_n)\, d\sigma.$$

Hence, we have proved (5.4).

We now show the convergence of e. Recall that, for any strictly interior dual element τ_i',

$$e_i = (\mathcal{D}'(E_e^0 - (E')_f^0))_i,$$

where

$$(E_e^0 - (E')_f^0)_r = \frac{1}{h_r} \int_{\sigma_r} \mathbf{E}(x, 0) \cdot \mathbf{t}_r\, dl - \frac{1}{s_r'} \int_{\kappa_r'} \mathbf{E}(x, 0) \cdot \mathbf{n}_r\, d\sigma.$$

Taking a point $Q \in \sigma_r \cap \kappa_r'$, we have

$$\begin{aligned}(E_e^0 - (E')_f^0)_r &= \frac{1}{h_r} \int_{\sigma_r} (\mathbf{E}(x, 0) - \mathbf{E}(Q, 0)) \cdot \mathbf{t}_r\, dl - \frac{1}{s_r'} \int_{\kappa_r'} (\mathbf{E}(x, 0) - \mathbf{E}(Q, 0)) \cdot \mathbf{n}_r\, d\sigma \\ &= \frac{1}{h_r} \int_{\sigma_r} (\mathbf{E}_j(x, 0) - \mathbf{E}_j(Q, 0))\, dl - \frac{1}{s_r'} \int_{\kappa_r'} (\mathbf{E}_j(x, 0) - \mathbf{E}_j(Q, 0))\, d\sigma.\end{aligned}$$

for some j, $1 \le j \le 3$. By the mean value theorem,

$$|(E_e^0 - E_f^0)_r| = |\frac{1}{h_r} \int_{\sigma_r} \mathbf{E}_j'(\xi_1, 0)(x - Q)\, dl - \frac{1}{s_r'} \int_{\kappa_r'} \mathbf{E}_j'(\xi_2, 0)(x - Q)\, d\sigma| \le Ch,$$

where h is the maximum edge length of all elements and

$$C := \sum_{k=1}^{2} \|\mathbf{E}(x, 0)\|_{C^1(\Omega_k)^3}.$$

Similar arguments can be applied to show the convergence of the components in (5.9). □

We remark that the last term in (5.5) vanishes for any strictly interior dual element τ_i'. But for any interface dual element τ_j', we can integrate both sides of (2.3) over τ_j' and then apply the divergence theorem to obtain

$$\sum_{\kappa_r' \in \partial \tau_j'} \int_{\kappa_r'} \epsilon \mathbf{E} \cdot \mathbf{n}_r\, d\sigma = \int_{\tau_j'} \rho\, dx + \int_{\tau_j' \cap \Gamma} \rho_\Gamma\, d\sigma.$$

Thus (5.4) is a fully discrete approximation of this integral version of the divergence constraint (2.3).

Remark. The finite volume method and the theory of this paper can be easily extended to the case, where the domain Ω and its subdomain Ω_1 are both rectangular, and the primal and dual meshes consist of only rectangular elements, and to the case that Ω is a multiple-connected polyhedral domain.

6 Numerical Implementations

In this section, we apply the finite volume method (4.12)-(4.13) to solve the Maxwell's system (2.1)-(2.4) in the discontinuous media. It can be seen from the numerical examples below that the convergence of the scheme is of second order for the considered Maxwell's equations with discontinuous physical coefficients.

Let $\Omega \times [0,T] = [0,1]^3 \times [0,1]$ and $\Omega_1 = [\frac{1}{3}, \frac{2}{3}]^3$. We divide $[0,T]$ into N_T equal subintervals and triangulate the domain Ω into non-uniform cuboids in the following way. First, the number of subintervals in each axis direction is the same, denoted by N. Next, in each axis direction, two consecutive subintervals are paired up and have a prescribed ratio. In the following example, the corresponding ratios for x-, y- and z-axis are $1:2$, $2:3$ and $4:3$ respectively. We also assume the media are equipped with the following discontinuous physical parameters:

$$\epsilon = \begin{cases} 0.1 & \text{in } \Omega_1 \\ 2 & \text{in } \Omega_2 \end{cases}, \qquad \mu = \begin{cases} 0.05 & \text{in } \Omega_1 \\ 1 & \text{in } \Omega_2 \end{cases}$$

To check the accuracy of the finite volume method (4.12)-(4.13), we construct the Maxwell's system (2.1)-(2.4) with its exact solutions given by

$$\mathbf{E} = \begin{bmatrix} -e^{\pi t}\cos(2\pi x)\sin(2\pi y)\sin(2\pi z) \\ -e^{\pi t}\sin(2\pi x)\cos(2\pi y)\sin(2\pi z) \\ -e^{\pi t}\sin(2\pi x)\sin(2\pi y)\cos(2\pi z) \end{bmatrix}$$

$$\mathbf{B} = \begin{bmatrix} -0.05\cos(2\pi x)\sin(2\pi y)\sin(2\pi z) + x \\ -0.05\sin(2\pi x)\cos(2\pi y)\sin(2\pi z) - y \\ -0.05\sin(2\pi x)\sin(2\pi y)\cos(2\pi z) + 1 \end{bmatrix}$$

We note that both $\mathbf{E}$ and $\mathbf{B}$ are continuous in Ω, but $\mathbf{H} = \frac{1}{\mu}\mathbf{B}$ and $\mathbf{D} = \epsilon\mathbf{E}$ are discontinuous across the interface. We can verify that the exact solution $(\mathbf{E}, \mathbf{B})$ satisfies the interface conditions $[\mathbf{E} \times \mathbf{m}] = 0$ and $[\mathbf{B} \cdot \mathbf{m}] = 0$. Solving the fully discrete finite volume system (4.12)-(4.13), we obtain the following result:

N_T	N	error	ratio
180	6	2.1273	—
360	12	0.7521	2.83
720	24	0.2100	3.58
1440	48	0.0543	3.86
2880	96	0.0140	3.88

Table 1: Convergence rate for the first example

The errors shown in the table are the discrete L^2-norm errors between the true solution $(\mathbf{E}, \mathbf{B})$ and the finite volume solution (E, B), namely

$$\max_{0 \le n \le N_T - 1} \left\{ \|\mathbf{E}^n - E^n\|_{W'} + \|\mathbf{B}^{n+1/2} - B^{n+1/2}\|_W \right\}.$$

where $\|\cdot\|_{W'}$ and $\|\cdot\|_W$ are the norms induced by the scalar products in (3.1) and (3.2) respectively. From the table above, we see that the convergence rate is approximately $O(h^2)$, that indicates the second order accuracy of the proposed finite volume method (4.12)-(4.13).

Our second example is concerned with the Maxwell's system (2.1)-(2.4) with the following true solutions

$$\mathbf{E_1} = \begin{bmatrix} -e^{\pi t}\cos(6\pi x)\sin(6\pi y)\sin(6\pi z) + \cos(2\pi x)\sin(2\pi y)\sin(2\pi z) \\ -e^{\pi t}\sin(6\pi x)\cos(6\pi y)\sin(6\pi z) + \sin(2\pi x)\cos(2\pi y)\sin(2\pi z) \\ -e^{\pi t}\sin(6\pi x)\sin(6\pi y)\cos(6\pi z) + \sin(2\pi x)\sin(2\pi y)\cos(2\pi z) \end{bmatrix}$$

$$\mathbf{E_2} = \begin{bmatrix} -(e^{\pi t}+1)\cos(6\pi x)\sin(6\pi y)\sin(6\pi z) + \cos(2\pi x)\sin(2\pi y)\sin(2\pi z) \\ -(e^{\pi t}+1)\sin(6\pi x)\cos(6\pi y)\sin(6\pi z) + \sin(2\pi x)\cos(2\pi y)\sin(2\pi z) \\ -(e^{\pi t}+1)\sin(6\pi x)\sin(6\pi y)\cos(6\pi z) + \sin(2\pi x)\sin(2\pi y)\cos(2\pi z) \end{bmatrix}$$

where $\mathbf{E}_i = \mathbf{E}|_{\Omega_i}$, for $i = 1, 2$, and $\mathbf{B}$ is the same as above. In this example, $\mathbf{H}$ field and the normal component of $\mathbf{E}$ is discontinuous across the interface Γ. Solving the system with the finite volume method (4.12)-(4.13) using uniform triangulation, i.e., all the three ratios corresponding to the three axis directions are $1:1$, we obtain the following result:

N_T	N	error	ratio
360	12	1.6090	—
720	24	0.4851	3.32
1440	48	0.1312	3.70
2880	96	0.0341	3.85
5760	192	0.0087	3.92

Table 2: Convergence rate for the second example

We see that the convergence rate is $O(h^2)$, which again demonstrates the second order accuracy of the numerical method (4.12)-(4.13).

We now present a numerical experiment for an electromagnetic scattering problem by our finite volume method using a uniform mesh. Assume that a plane wave source is given on the boundary $x = 0$. We choose the source as given by

$$E_y = \sin(4\pi(x - c_2 t)), \quad H_z = \epsilon_2 c_2 \sin(4\pi(x - c_2 t))$$

where $c_2 = (\epsilon_2\mu_2)^{-\frac{1}{2}}$ is the speed of light in the medium occupied by Ω_2. Note that both the electric and magnetic fields propagate in the x-direction. The numerical solution of the electric field E_y is shown in the following figure:

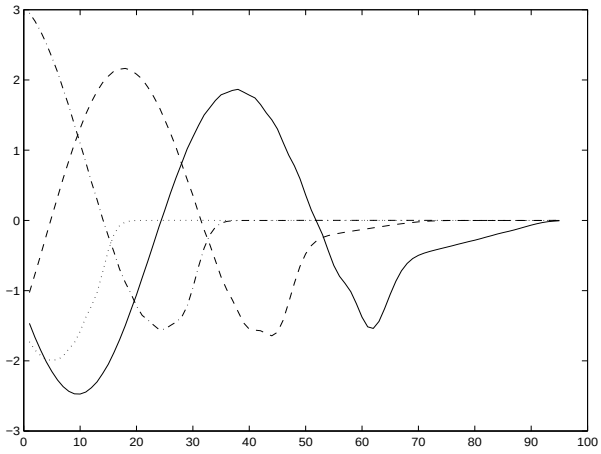

Figure 3: Numerical solution of E_y

where in figure 3 the dotted line, dash dot line, dash line and solid line represent respectively the snap shots of the electric field patterns at times $t = 0.25, 0.5, 0.75, 1$. In addition, the vertical axis denotes the amplitude of the field strength while the horizontal axis denotes the position in x-direction. We remark that the amplitudes of the waves have been doubled so that it looks clearer. The plot in figure 3 corresponds to the pattern of the electric field which does not pass through the inhomogeneous part of Ω, that is Ω_1. It shows that the electric field propagates smoothly in the x-direction.

In the following figure, we give the numerical solution of the magnetic flux density B_z:

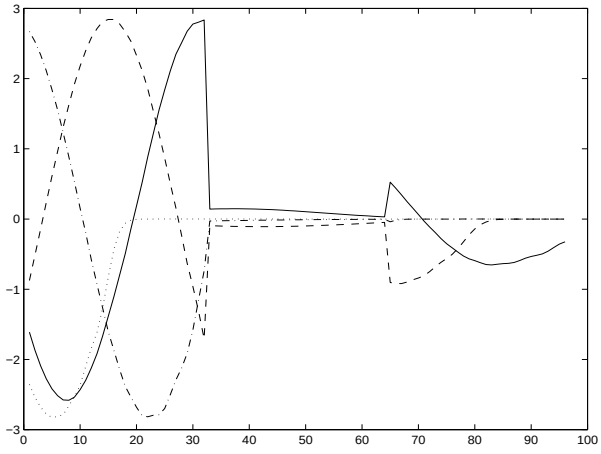

Figure 4: Numerical solution of B_z

where we have shown the snap shots of patterns of the magnetic flux density which passes through the inhomogeneous part of Ω, that is Ω_1. From the figure, we see that the wave propagates in the x-direction, but there are discontinuities when the wave passes through the interface between Ω_1 and Ω_2. We remark that the amplitudes of the waves have been doubled and all the notations in figure 4 are defined similarly as figure 3.

References

[1] Z. Chen, Q. Du and J. Zou. *Finite element methods with matching and non-matching meshes for Maxwell equations with discontinuous coefficients.* SIAM J. Numer. Anal, 37 (2000), pp. 1542–1570.

[2] Z. Chen and J. Zou. *Finite element methods and their convergence for elliptic and parabolic interface problems.* Numerische Mathematik, 79 (1998), pp. 175-202.

[3] P. Ciarlet and J. Zou. *Fully discrete finite element approaches for time-dependent Maxwell's equations.* Numerische Mathematik, 82 (1999), pp. 193-219.

[4] J. Jin. *The finite element method in electromagnetics.* John Wiley and Sons, Inc.

[5] Z. Li and J. Zou. *Theoretical and numerical analysis on a thermo-elastic system with discontinuities.* J. Comput. Appl. Math., 92 (1998), pp. 37-58.

[6] N. K. Madsen. *Divergence preserving discrete surface integral methods for Maxwell's curl equations using non-orthogonal unstructured grids.* J. Comput. Phys., 119 (1995), pp. 34-45.

[7] P. Monk and E. Süli. *A convergence analysis of Yee's scheme on nonuniform grids.* SIAM J. Numer. Anal., 31 (1994), pp. 393-412.

[8] R. A. Nicolaides. *Direct discretization of planer div-curl problems.* SIAM J. Numer. Anal., 29 (1992), pp. 32-56.

[9] R. A. Nicolaides and D. Q. Wang. *Convergence analysis of a covolume scheme for Maxwell's equations in three dimensions.* Math. Comp., 67 (1998), pp. 947-963.

[10] R. A. Nicolaides and X. Wu. *Covolume solutions of three-dimensional div-curl equations.* SIAM J. Numer. Anal., 34 (1997), pp. 2195-2203.

[11] A. Taflove. *Computational electrodynamics.* Artech House, Inc., 1995.

[12] K. S. Yee. *Numerical solution of initial boundary value problems involving Maxwell's equations in isotropic media.* IEEE Trans. Antennas Propagat., 14 (1966), pp. 302-307.

[13] K. S. Yee and J. S. Chen *The finite-difference time-domain and the finite-volume time-domain methods in solving Maxwell's equations.* IEEE Trans. Antennas Propagat., 45 (1997), pp. 354-363.